Expression of an additional cathelicidin antimicrobial peptide protects against bacterial skin infection

Phillip H. A. Lee*[†], Takaaki Ohtake[†‡], Mohamed Zaiou*, Masamoto Murakami[§], Jennifer A. Rudisill*, Kenneth H. Lin*, and Richard L. Gallo*[¶]

*Division of Dermatology, University of California at San Diego, and Veterans Affairs San Diego Healthcare Center, San Diego, CA 92161; and [‡]Third Department of Internal Medicine and [§]Department of Dermatology, Asahikawa Medical College, Asahikawa 078-8307, Japan

Cathelicidin antimicrobial peptides are effectors of innate immune defense in mammals. Humans and mice have only one cathelicidin gene, whereas domesticated mammals such as the pig, cow, and horse have multiple cathelicidin genes. We hypothesized that the evolution of multiple cathelicidin genes provides these animals with enhanced resistance to infection. To test this, we investigated the effects of the addition of cathelicidins by combining synthetic cathelicidin peptides *in vitro*, by producing human keratinocytes that overexpress cathelicidins in culture, or by producing transgenic mice that constitutively overexpress cathelicidins *in vivo*. The porcine cathelicidin peptide PR-39 acted additively with human cathelicidin LL-37 to kill group A *Streptococcus* (GAS). Lentiviral delivery of PR-39 enhanced killing of GAS by human keratinocytes. Finally, transgenic mice expressing PR-39 under the influence of a K14 promoter showed increased resistance to GAS skin infection (50% smaller necrotic ulcers and 60% fewer surviving bacteria). Similarly constructed transgenic mice designed to overexpress their native cathelicidin did not show increased resistance. These findings demonstrate that targeted gene transfer of a xenobiotic cathelicidin confers resistance against infection and suggests the benefit of duplication and divergence in the evolution of antimicrobial peptides.

innate immunity | keratinocyte

Bacterial resistance to conventional antibiotics has become commonplace, resulting in escalating numbers of life-threatening infections (1–5). Recent studies of cationic peptides as mediators of innate host defense have shown that, unlike pharmacologic antibiotics, these native host defense molecules have maintained broad-spectrum antimicrobial activity and resisted most microbial strategies for resistance (6, 7). These observations suggest that antimicrobial peptides may be attractive alternatives to current antibiotic regimens in select disease situations.

Cathelicidins are a diverse family of cationic peptides with broad-range antimicrobial ability. Whereas humans and rodents have a single cathelicidin, many mammals have duplicated the cathelicidin gene to produce several unique C-terminal antimicrobial peptides with structures that vary from α-helical to β-sheet to rich in single amino acids (8–10). It is unknown whether the presence of multiple cathelicidins found in animals such as the pig and cow provides a benefit to these mammalian species. However, mice generated to be deficient in their sole cathelin-related antimicrobial peptide (mCRAMP) develop significantly larger group A *Streptococcus* (GAS) skin lesions, compared with their wild-type littermates (11), and inhibiting activation of antimicrobial peptides increases bacterial growth in pigs (12) and mice (13). Taken together, these observations support an essential role for antimicrobial peptides in defense against infection.

In systems with relative deficiencies of antimicrobial peptide function, prior studies have suggested that gene transfer technology for antimicrobial peptides could be beneficial (14). However, antimicrobial peptides also affect the host, stimulating cell behaviors such as chemotaxis and angiogenesis (15, 16). Thus, limiting activation of antimicrobial peptides to sites of infection would be

desirable. To address this, we investigated the consequences of expressing structurally distinct cathelicidins in their precursor form. Furthermore, we compared the relative benefit of expressing more native cathelicidin with that of expressing an additional and distinct pig cathelicidin in mice. Our data suggest that delivery of additional native cathelicidin is ineffective, but expression of a xenobiotic cathelicidin as a propeptide is an effective mechanism for conferring enhanced resistance against bacterial infection in skin.

Methods

Synthetic Porcine Cathelicidin Peptide PR-39. The C-terminal peptide form of PR-39 was synthesized (Quality Control Biochemicals, Hopkinton, MA) and found to be 99% pure by HPLC and endotoxin-free by *Limulus* Amebocyte Lysate assay (Associates of Cape Cod).

Antimicrobial Activity Assays. For solution killing assays, GAS strain NZ131 (17) was grown in tryptic soy broth (TSB) (Sigma), and 10,000 bacteria [OD_{600} 1.0 corresponds to 2.5×10^8 colony-forming units (CFU)/ml] were incubated with various concentrations of PR-39 and/or mCRAMP in 100 μl of TSB overnight at 37°C. Bacterial counts were determined by optical density at 600 nm. CFU/ml was determined after plating samples overnight on TSB agar. To examine the efficacy of pLV/PR-39-modified HaCaT cells to kill bacteria, transduced cells were washed three times with PBS, harvested in 100 μl of distilled water, and subjected to mild sonication. A total of 10,000 bacteria (diluted from logarithmic-phase growth, OD_{600} 0.6) were mixed with 10 μl of cell lysates in a total volume of 50 μl of TSB and incubated at 37°C overnight. Surviving CFU/ml was determined as described.

Cathelicidin Lentivirus Production. Pig cathelicidin cDNA corresponding to either mature PR-39 peptide or the full-length PR-39 precursor (signal peptide plus cathelin plus PR-39) was amplified by using PCR and inserted into pLenti6/V5/TOPO vector (Invitrogen), generating the following constructs: pLV/PR-39 and pLV/FL-PR-39 containing precursor full-length PR-39 or mature PR-39 under control of a cytomegalovirus promoter. Insertion and orientation of cathelicidin genes were confirmed by plasmid sequencing. Constructs were cotransfected with a mixture of packaging plasmids pLP1, pLP2, and pLP/VSV-G into human embryonic kidney cells (293 T cells). Transfections of 293 T cells (1.5×10^6) were carried out by using Lipofectamine (GIBCO) in serum-free medium. After 12 h, the medium was replaced with complete medium, and cells were further incubated for 72 h. Viral supernatant was collected and filtered (0.45-μm filter). pLV-B-gal expressing β-gal was used as positive control. Expression of β-gal was

---

scored by X-Gal staining. Titers were calculated by counting the number of foci of blue cells per well and dividing the count by the dilution factor. When titered in the human keratinocyte cell line HaCaT, titer for the control pLV/LacZ vector, was ≈5 × 10^{7} transducing units/ml. pLV/PR-39 and pLV/FL-PR-39 were similarly produced by transient transfection 293 cells. Viral stocks were stored frozen at −80°C.

HaCaT Cell Transduction. For transduction with lentivirus stock, HaCaT cells were grown in six-well plates to 30–50% confluence. Before infection, the medium was replaced by serum-free medium supplemented with 8 μg/ml Polybrene. After addition of conditioned medium (300 μl) from 293 cells infected with PR-39, full-length PR-39, or LacZ vector, cells were incubated at 37°C overnight. The next day, the medium was changed to a growth medium without Polybrene. After expansion in culture for 48–72 h, HaCaT cells were collected and analyzed for cathelicidin expression. Transduction efficiency was analyzed by visualization of β-gal expression in controls.

Subcutaneous Application of PR-39. Wild-type littermates of transgenic mice were prepared by shaving and chemical depilation (Neet, Whitehall Laboratories, New York) of back hair. In a blinded fashion, mice were injected s.c. with either 320 μM synthetic PR-39 or 1× PBS three times per day for 10 days. Biopsies of injection sites were taken and prepared for sectioning by formalin-fixation and paraffin-embedding. Hematoxylin/eosin-stained sections were analyzed by studying 10 separate high-power fields for each section. Representative digital images were taken. All animal procedures were approved by the Veterans Affairs San Diego Healthcare System subcommittee on animal studies (protocol no. 02-037).

Construction of Transgenes and Production of Transgenic Mice. A *Bgl*II restriction fragment of a TOPO TA vector (Invitrogen) including the full-length PR-39 or full-length mCRAMP cDNA was inserted into the *Bam*HI restriction site of a pG3Z-K14 cassette containing a keratin 14 promoter (18). Transgenic mice were produced by microinjection of the transgene constructs into fertilized embryos before implantation in pseudopregnant mice as described in ref. 19 (Transgenic Core Facility, University of California at San Diego). For each transgene construct, at least two independent transgenic mouse lines were identified and established. One strain was backcrossed to C57BL/6 at seven generations for the coisogenic strain. Its genetic background was 97% C57BL/6 by microsatellite chromosomal location. Another strain was backcrossed to BALB/c at five generations.

Identification of K14-Cathelicidin Transgenic Mice. Genomic DNA from mouse tail tissue was purified by using the Wizard Genomic DNA purification kit (Promega). For screening, PCRs were run with 5 ng of genomic DNA and 200 nM oligonucleotide pairs K14PR39F (5′-TCAGATCTGCACCATGGAGACCCAGA-3′) and K14PR39R (5′-ACAGATCTACCGTTTTCCGGGGAACC-3′) for PR-39 and CRAMPK14F (5′-AGGAGATCTTGGGAAC-CATGCAGTT-3′) and CRAMPK14R (5′-GCAGATCTACT-GCTCCGGCTGAGGTA-3′) for mCRAMP by using Platinum PCR SuperMix (GIBCO/BRL) in a 25-μl reaction volume. Transgene integration status was analyzed by Southern blotting. Mouse tail genomic DNA (10 μg) was digested with *Hin*dIII restriction enzyme, subjected to Southern blotting and hybridization by using Hybond N+ nylon membrane (Amersham Pharmacia), and probed with ^{32}P-labeled PR-39 or mCRAMP cDNA.

RT-PCR. Total RNAs were extracted from HaCaT keratinocytes or mouse skin as described in ref. 20. cDNAs were made from 1 μg of total RNA with 500 ng of oligo(dT) primer and SuperScript II RNase H⁻ Reverse Transcriptase (GIBCO/BRL) at 42°C for 1 h.

For HaCaT cells, PCR amplification was done by using the oligo set PR-39–5-Lentv (5′-CACCATGGAGACCCAGAGGGCCAG-3′) and PR-39–3-Lentv (5′-CTATCACCGTTTTCCGGGGAAC-CGTGG-3′) for full-length PR-39 and pLentv-PR-39p-5 (5′-CACCATGAGGAGACTGCCCCGACCCCCATAT-3′) and PR-39–3-Lentv for mature PR-39 peptide. For transgenic mice, PCR amplification was done by using the oligo set K14PR39F and K14PR39R for PR-39 and CRAMPK14F and CRAMPK14R for mCRAMP mice. For confirmation of PCR products, bands of expected size were sequenced.

Immunohistochemistry. Immunostaining was done following a protocol described in ref. 21, except for the following differences: Sections were made of frozen skin tissue from day 1 newborn mice. Primary antibody was 1:500 diluted affinity-purified rabbit anti-PR-39, whereas secondary antibody was 1:200 diluted biotinylated goat anti-rabbit. Sections were counterstained with hematoxylin QS (Vector Laboratories). Antibody specificity was confirmed by the use of rabbit nonimmune IgG. Additional staining for syndecan-1 (rat anti-mouse syndecan-1, 281-2), blood vessels (anti-CD31, BD Biosciences), and leukocytes (anti-CD45, BD Biosciences) were done following the manufacturer's instructions.

Western Blot Analysis. K14-Cath-PR-39 transgenic mice and their wild-type littermates were anesthetized, had their back hair removed, and received either a 1-cm full-thickness incision or inoculation with GAS (as described in *Methods* for mouse model of GAS infection). On day 4 after either incision or inoculation, a 2-mm area surrounding the wound or lesion was excised, weighed, diced, and homogenized for 10 min with a Dounce homogenizer in 1 ml of 1 M HCl and 1% trifluoroacetic acid on ice. Homogenized tissues in solution were then rotated for 3 days at 4°C. After centrifugation at 40,000 × g at 4°C for 30 min, supernatants were transferred to new tubes and lyophilized completely. For extracts from wounded skin, the resulting protein pellets were dissolved with distilled water to obtain a final protein concentration of 0.8 mg of tissue per μl. For extracts from infected lesions, samples were resuspended in 500 μl of PBS and, after the addition of 50 μl of rabbit anti-PR-39 antibody, were incubated at 4°C with shaking for 1 h. Fifty microliters of protein A-agarose beads (Boehringer Mannheim) was added, and samples were incubated at 4°C with shaking overnight. Samples were then centrifuged at 4,500 rpm for 2 min in an Eppendorf 5415C centrifuge, washed three times with PBS, and then resuspended in 50 μl of pH 8.45 Tris/Tricine sample buffer. All extracts were boiled in Tris/Tricine sample buffer (Bio-Rad) containing 5% 2-mercaptoethanol for 10 min and incubated at 37°C overnight before electrophoresis. An extract from pig bone marrow was used as a positive control. Proteins were separated by means of Tris/Tricine/SDS/16.5% PAGE and then transferred to a poly(vinylidene difluoride) Immobilon P membrane (Millipore). The membrane was blocked with 10% nonfat dry milk/0.1% Tween 20 in Tris-buffered saline, pH 7.6 at room temperature for 3 h, incubated at 4°C overnight with rabbit anti-PR-39 antibody (dilution 1:1,000), and then incubated at room temperature for 1 h with goat anti-rabbit antibody/horseradish peroxidase (Dako) diluted 1:4,000. Western Lightning chemiluminescence reagent (Perkin–Elmer) was used to detect electrochemiluminescence.

Quantitative Real-Time PCR. RNA from mouse skin was extracted by using TRIzol reagent (Invitrogen). After DNase digestion, RNA samples were passed through RNeasy Mini Spin columns for RNA Cleanup (Qiagen). RT-PCR was performed on 2 μg of RNA by using the Retroscript kit (Ambion, Austin, TX). Real-time PCR was performed by using an ABI Prism 7000 sequence detection system from Applied Biosystems. GAPDH-F (5′-CTTAGCAC-CCCTGGCCAAG-3′) and GAPDH-R (5′-TGGTCATGAGTC-

CTTCCACG-3′) were used to amplify GAPDH, and mCRAMP-F (5′-CTTCAACCAGCAGTCCCTAGACA-3′) and mCRAMP-R (5′-TCCAGGTCCAGGAGACGGTA-3′) were used to amplify mCRAMP. A 1-μl reverse transcriptase reaction was added to 24 μl of SYBR Green PCR Master Mix (Applied Biosystems) and 0.25 μl of each 20 μM primer. The thermal profile was as follows: 50°C for 2 min, 95°C for 10 min, and 40 $\times$ (95°C for 15 s, 60°C for 1 min). The melting temperature profile of amplicons was determined to show the specificity of amplification. Results were analyzed by using the Comparative Ct method, where ΔCt = Ct (mCRAMP) − Ct (GAPDH) and $\Delta\Delta$Ct = ΔCt (K14-Cath-mCRAMP mice) − ΔCt (wild-type mice). Relative expression was calculated as $2^{-(\Delta\Delta Ct)}$. All real-time PCRs reactions were performed in triplicate.

Mouse Model of GAS Infection. GAS invasiveness in mouse skin was measured by modification of a GAS infection model described in refs. 11 and 22. All mice in the GAS infection experiment were C57BL/6 background mice. Sex-matched transgenic mice and their wild-type littermates were injected s.c. with 200 μl of a 50/50 suspension of Cytodex Microcarrier beads (Aldrich) and GAS NZ131 (OD$_{600}$ = 0.9). Lesion sizes were measured on day 4 after inoculation. Wound tissue excised on day 4 after infection was homogenized in 25 mg of tissue per ml of PBS. Aliquots of homogenate were serially diluted and plated on blood agar. CFU count was determined after overnight incubation at 37°C. Histological sections were fixed in 10% buffered formalin, embedded in paraffin, and stained with hematoxylin/eosin.

Statistical Analysis. Student's t test was used for statistical analysis. Differences in values were considered significant when $P < 0.05$.

Results

PR-39 Enhances mCRAMP Killing of GAS. The combined activity of PR-39 and mCRAMP peptides was tested against GAS. GAS was selected because of the large inflammatory response it induces in skin, prior work showing it to be a sensitive system for detecting the activity of the native mouse catholicidin, and its importance as a human skin pathogen. Antimicrobial activity was assessed after incubation with various concentrations of PR-39 and mCRAMP. A solution killing assay showed that subbactericidal doses of PR-39 enhanced the inhibitory (Fig. 1A) and bactericidal (Fig. 1B) activity of mCRAMP against GAS. These observations supported the use of PR-39 in further studies as a potential supplemental cathelicidin.

Expression of PR-39 Confers Antimicrobial Activity to Keratinocytes. To investigate the functional consequences of a supplemental cathelicidin in cells, the human keratinocyte cell line HaCaT was infected with lentiviral expression constructs engineered to express the pig cathelicidin PR-39 in its full-length precursor or mature peptide form. Expression of the mRNA encoding the full-length and mature forms was verified by using RT-PCR (Fig. 2A). Previous studies have suggested that the antimicrobial and host-signaling effects of cathelicidin peptides are activated upon processing of the precursor protein (23). Consistent with these studies, GAS was killed in the presence of extracts from keratinocytes expressing the mature peptide form of PR-39 but not from those that expressed PR-39 in its native precursor form (Fig. 2B). These observations confirmed the requirement for processing of cathelicidin to activate antimicrobial activity and the efficacy of PR-39 antimicrobial activity when expressed in human keratinocytes along with their native cathelicidin and other antimicrobial molecules.

Effect of PR-39 on Mouse Skin. PR-39 is multifunctional, acting to kill microbes as well as influencing chemotaxis, angiogenesis, and extracellular matrix synthesis (15, 16, 24). This activity was evaluated by s.c. injection of PR-39 into normal mouse skin over 10 days. Histological analysis of the site of injection revealed a distinct increase in leukocytic infiltrate that was not observed at control
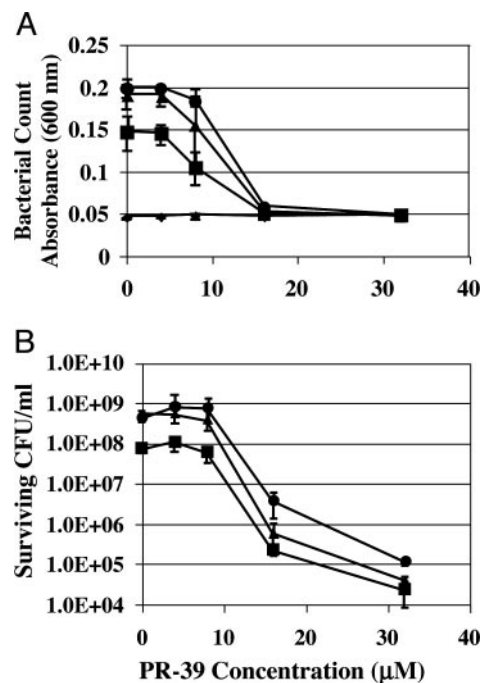

Fig. 1. PR-39 enhances killing of GAS by mCRAMP. The antimicrobial activity of PR-39 and mCRAMP was evaluated by solution killing assay. GAS was incubated with increasing concentrations of PR-39 and 0 μM (●), 1 μM (▲), 4 μM (■), and 8 μM (◆) mCRAMP. (A) Bacterial counts decreased when GAS was incubated with the combination of PR-39 and mCRAMP. (B) CFU determination shows a corresponding decrease in live bacteria. Data shown are means (±SD) from triplicate determination representative of two independent experiments.

sites identically injected with vehicle alone (data not shown). These observations suggested that an inflammatory host response to the mature peptide gene product could confound the interpretation of antimicrobial gene delivery to skin.

Production and Characterization of Cathelicidin Transgenic Mice. To investigate the effect of multiple structurally distinct cathelicidin peptides, transgenic mice were generated that expressed the precursor form of PR-39 or mCRAMP in basal keratinocytes. Full-length cathelicidins were prepared with the whole ORF cDNA and subcloned into an expression vector containing the human K14 promoter/enhancer and K14 polyadenylation signal sequence (Fig. 3 A and B). Southern blot analysis confirmed successful addition of the transgene in multiple independent mouse lines (data not shown). Expression of PR-39 or mCRAMP mRNA was verified by using RT-PCR (Fig. 3 C and D). Two different founder lines with detectable expression were selected for further experiments.

Antibody to PR-39 confirmed protein expression in the epidermis and outer root sheath of hair follicles of K14-Cath-PR-39 transgenic mice (Fig. 3E), whereas wild-type mouse skin lacked detectable staining (Fig. 3F). Protein extracts were next assayed from wounded mouse skin, a setting where cathelicidins are known to be induced (23). Western blot analysis showed a band corresponding to the precursor form of PR-39 in the extract from wounded K14-Cath-PR-39 transgenic mouse skin, whereas wild-type mouse skin lacked any bands (Fig. 3G). PR-39 antibody immunoprecipitation of extracts from GAS-infected mouse skin allowed for visualization of bands corresponding to the precursor and mature forms of PR-39 (Fig. 3G). In addition to immunodetection of mCRAMP (data not shown), expression of K14-Cath-mCRAMP mRNA in transgenic mice was confirmed by using
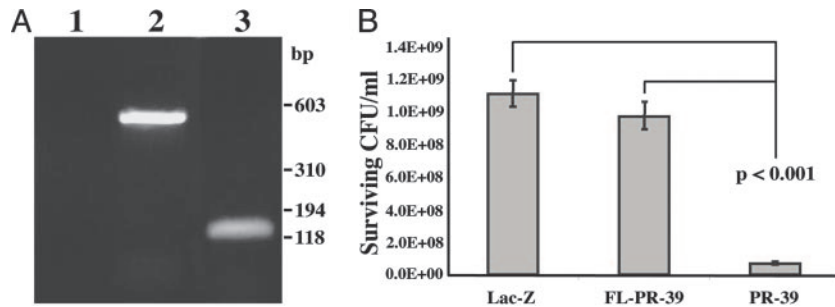
Fig. 2. Lentiviral delivery of PR-39 to HaCaT cells confers antimicrobial activity. (*A*) RT-PCR analysis for the presence of full-length or mature PR-39 mRNA in transduced cells. Lanes: 1, negative control (HaCaT cells, no transduction); 2, full-length PR-39-transduced HaCaT cells (450-bp product); 3, mature PR-39-transduced HaCaT cells (120-bp product). Expression of cathelicidins in HaCaT cells was verified 72 h after infection with viral particles. (*B*) *Ex vivo* assessment of cathelicidin-mediated killing of bacteria by PR-39-expressing HaCaT cells. Cell lysates prepared from pLV/LacZ-, pLV/FL-PR-39-, or pLV/PR-39-infected HaCaT cells were incubated overnight with GAS NZ131. Antimicrobial activity of each construct against GAS was determined by CFU counts. Data shown are means (±SD) of six samples and are representative of two independent experiments.

quantitative real-time PCR showing ≈18-fold more mCRAMP mRNA in transgenic mice than in wild-type controls (Fig. 3*H*).

Expression of Pig Cathelicidin in Mouse Skin Augments Protection Against GAS. In the gut of mice, transgenic delivery of a human α-defensin provides protection against salmonellosis, but no analysis of the effects of constitutive overexpression of this antimicrobial gene or of native α-defensin was performed (25).

With the confirmation of mouse lines effectively overexpressing either K14-Cath-PR-39 or K14-Cath-mCRAMP, it became possible to evaluate the effects of native vs. xenobiotic antimicrobial peptides. None of the mouse lines produced showed any change in skin morphology during development or under resting conditions housed in an aseptic environment. Histological evaluation of the skin lacked evidence of the leukocytic infiltrate, although injection of synthetic PR-39 peptide in mouse skin did

<div style="text-align: right;">IMMUNOLOGY</div>
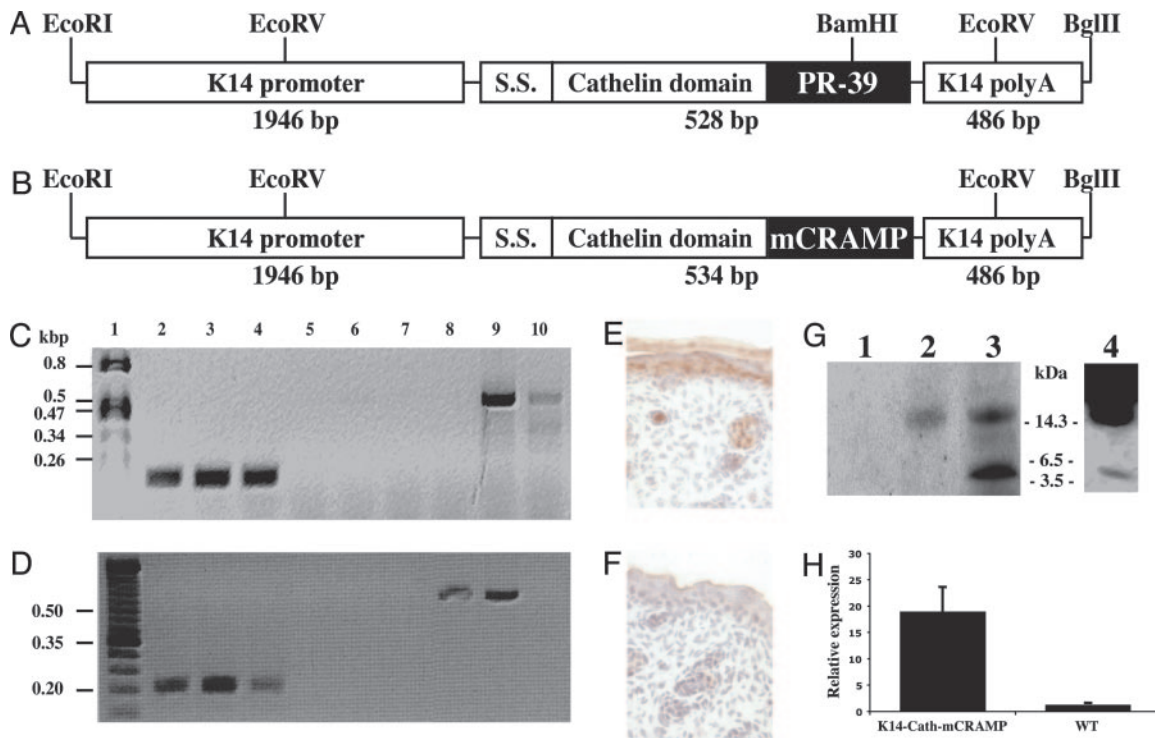
Fig. 3. Construct of K14-Cath-PR-39 and K14-Cath-mCRAMP transgenic mice. (*A* and *B*) Schematic representation of the K14-Cath-PR-39 (*A*) and K14-Cath-mCRAMP (*B*) transgene constructs. RT-PCR analysis was performed on total RNA extracted from skin of adult mice. S.S., signal sequence. (*C*) RT-PCR analysis verifying PR-39 transcription. Lanes: 1, DNA marker; 2, 5, and 8, wild-type littermate; 3, 6, 9, and 4, 7, and 10, two different founder K14-PR-39 transgenic mice, respectively; 2–4, β-actin amplification; 5–7, PR-39 amplification without reverse transcriptase reaction; 8–10, PR-39 amplification. (*D*) RT-PCR analysis verifying mCRAMP transcription. Lanes: 1, DNA marker; 2, 5, and 8, and 3, 6, and 9, and 4, 7, and 10, three different founder K14-mCRAMP transgenic mice, respectively; 2–4, β-actin amplification; 5–7, mCRAMP amplification without RT reaction; 8–10, mCRAMP amplification. (*E* and *F*) Frozen skin sections from day 1 newborn K14-Cath-PR-39 transgenic (*E*) and wild-type (*F*) mice fixed in 4% paraformaldehyde and processed for immunohistochemical stain by using a polyclonal antibody against PR-39. (×40.) (*G*) Western blot analysis of protein extracts from wounded wild-type mouse skin (lane 1), wounded K14-Cath-PR-39 transgenic mouse skin (lane 2), pig bone marrow as a control (lane 3), or GAS-infected K14-Cath-PR-39 mouse skin after immunoprecipitation with PR-39 antibody (lane 4). The blot was probed with a polyclonal antibody against PR-39. (*H*) Quantitative real-time PCR for mCRAMP expression in K14-Cath-mCRAMP mouse skin, compared with their littermate controls. Data are means (±SD) of four mice from each group.

induce a mild lymphocytic infiltrate (data not shown). Other phenomena previously seen in PR-39 transgenic animals, like angiogenesis (16), also were absent. Furthermore, after full-thickness aseptic injury, no difference in inflammation, reepithelialization, angiogenesis, or wound closure was observed in transgenic mice, compared with their wild-type littermates.

Both lines of each of the cathelicidin transgenic mice were then tested by using a model of GAS skin infection. *In vivo* processing enzymes during infection activate native cathelicidin precursors upon challenge (23), therefore providing a mechanism for enabling activation of the precursor transgene product. After s.c. injection with GAS, K14-Cath-mCRAMP mice did not show any significant difference in the area of necrotic ulcer, compared with wild-type mice (Fig. 4*A*). However, when K14-Cath-PR-39 transgenic mice were inoculated, necrotic lesion size was significantly smaller than in wild-type mice ($P < 0.05$, Fig. 4 *B–D*). Similar results were seen in both transgenic lines. Histological analysis of skin during infection showed no appreciable difference in leukocyte infiltrate, compared with controls (Fig. 4 *E* and *F*). To test whether the resistance to infection in K14-Cath-PR-39 transgenic animals correlated with increased bacterial killing, bacteria from necrotic lesions were isolated and plated. CFU determination showed that significantly fewer GAS grew from K14-Cath-PR-39 transgenic mice lesions, compared with wild-type mice ($P = 0.01$, Fig. 4*G*). In contrast, no significant difference was seen in CFU determination of GAS from K14-Cath-mCRAMP transgenic mice lesions, compared with controls (data not shown).

Discussion

Decreased cathelicidin expression in humans and mice has been associated with increased susceptibility to infection (11, 26). Other mammalian species, such as pig, cow, horse, sheep, and rabbit, differ from humans and mice in that they possess several distinct cathelicidin genes. We sought to determine whether acquisition of an additional cathelicidin gene would correspond to increased antimicrobial resistance, therefore explaining the benefit of cathelicidin gene duplication seen in many mammalian species other than human. This study demonstrates that targeted gene transfer of a pig antimicrobial peptide precursor to mouse skin protects against invasive bacterial infection by GAS.

The pig cathelicidin PR-39 has antimicrobial activity against a broad range of microorganisms (27) and was chosen for this study because of its unique structure, compared with human and mouse members of this gene family. This distinct structure adds to its potential to act additively with the native mouse cathelicidin. A solution killing assay confirmed that PR-39 enhanced the ability of mCRAMP to kill GAS and gave *in vitro* support for our hypothesis that the addition of a structurally distinct cathelicidin could be beneficial *in vivo*.

Next, a lentiviral system was used to express PR-39 in human HaCaT keratinocytes and to test the influence of PR-39 expression on bacterial killing by skin cells *ex vivo*. Like all other cathelicidins, PR-39 is initially made as a precursor consisting of a conserved cathelin domain and C-terminal peptide. Results demonstrated that only keratinocytes expressing the mature form of PR-39 had acquired the ability to kill GAS, whereas keratinocytes expressing the precursor form lacked this ability. This finding is consistent with previous reports that cathelicidin and defensin antimicrobial peptides require processing to become active (8, 13, 14, 23). These findings further supported the theory that adding an additional cathelicidin could confer enhanced resistance to bacterial infection and confirmed the requirement for processing of the precursor form.

Next, we physically delivered PR-39 peptide directly to skin to mimic the processed form of PR-39 found in pig wounds and expressed by our lentivirus-transfected keratinocytes. The injection of PR-39 induced a leukocyte infiltration at the injection site. Although the observed effect may reflect nonspecific toxicity of a
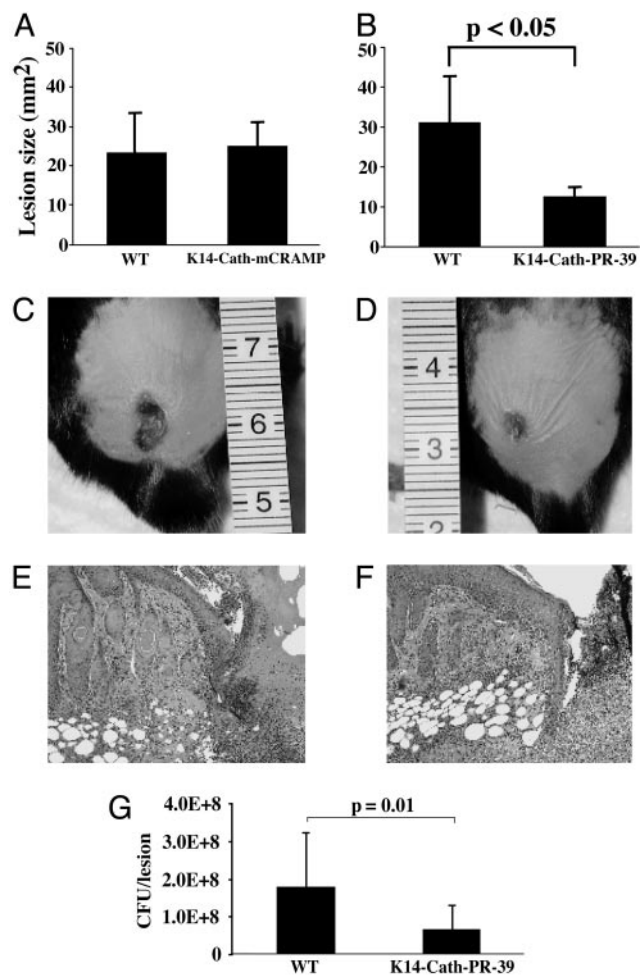
Fig. 4. K14-Cath-PR-39 transgenic mice are resistant to GAS infection. The area of necrotic ulcers in wild-type (WT) or transgenic mice was measured on day 4 after s.c. inoculation with GAS. (*A*) No difference in lesion size was seen between K14-Cath-mCRAMP transgenic and WT mice (data are means ± SD, representative of three independent experiments, $n = 18$ for WT and 14 for K14-Cath-mCRAMP transgenic mice). (*B*) K14-Cath-PR-39 transgenic mice had statistically smaller necrotic lesions, compared with WT mice (data are means ± SD, representative of three independent experiments, $n = 8$ for WT and 10 for K14-Cath-PR-39 transgenic mice). (*C* and *D*) WT (*C*) and K14-Cath-PR-39 transgenic mice (*D*) are shown on day 4 after s.c. inoculation with GAS. Representative images show the development of smaller lesions in K14-Cath-PR-39 transgenic mice. (*E* and *F*) Formalin-fixed, paraffin-embedded sections of infectious lesions from WT (*E*) and K14-Cath-PR-39 transgenic mice (*F*) show no appreciable difference in degree of leukocytic infiltrate in the center of the ulcer (hematoxylin/eosin-stained). (×100.) (*G*) CFU per lesion grown from GAS infectious lesions in WT and K14-Cath-PR-39 transgenic mice on day 4 after GAS inoculation. Lesions from K14-Cath-PR-39 transgenic mice had significantly fewer CFU, compared with lesions from WT mice (data are means ± SD and are representative of four separate experiments; $n = 12$ for WT and 12 for K14-Cath-PR-39 transgenic mice).

foreign peptide, our observations are consistent with host responses seen in prior studies in multiple systems (15, 16). Therefore, it appeared that the design of transgenic mice expressing the inactive precursor form of cathelicidins would be less likely to demonstrate confounding inflammation.

Mice designed to express the full-length PR-39 propeptide under control of the K14 promoter demonstrated no morphological phenotype before challenge. Conspicuously absent was evidence of an inflammatory response like that seen in skin treated with the mature PR-39 peptide. Because PR-39 induces the expression of syndecan-1, a proteoglycan important in wound repair (28), we also

tested whether K14-Cath-PR-39 transgenic mice displayed a difference in wound healing, compared with their wild-type littermates. No difference in speed of healing was observed. Similarly, although PR-39 is angiogenic in mice (16), no change in vessel formation was detectable in the transgenic animals. Several explanations may exist for the lack of phenotype, including insufficient expression, inability of the product expressed in basal keratinocytes to interact with target cells such as the fibroblasts or endothelial cells in the dermis, or lack of processing of the PR-39 precursor into sufficient amounts of the active mature peptide.

Only mice expressing the PR-39 precursor in their keratinocytes resisted GAS infection better than controls, whereas mice expressing the mCRAMP precursor showed no difference in lesion size. In the absence of an apparent increase in chemotaxis the most direct explanation for this effect is the innate antimicrobial activity of PR-39 or the cathelin pro-domain after cleavage. Both the cathelin and C-terminal portions of the human cathelicidin hCAP18/LL-37 are antimicrobial (8, 29). However, because the K14-Cath-mCRAMP mice also delivered increased cathelin pro-domain expression, the most likely explanation for resistance in K14-Cath-PR-39 mice, but not K14-Cath-mCRAMP mice, is the additive effect of PR-39 predicted by earlier experiments. Moreover, the observation that no difference was observed in K14-Cath-mCRAMP mice, compared with controls, suggests that the activity from native cathelicidin is maximal. An alternative explanation is that all lines of K14-Cath-mCRAMP express less peptide than K14-Cath-PR-39, but this seems less likely due to real-time PCR evidence of expression.

Although our data suggest that the increased resistance to skin infection seen in K14-Cath-PR-39 transgenic mice is due to enhancement of antimicrobial killing by the presence of PR-39, other explanations for this phenotype are still plausible. Expression of PR-39 may induce the release of cytokines, chemokines, or other native antimicrobial peptides, thereby indirectly conferring resistance to infection. An effect of PR-39 on the growth of endogenous flora also has not been ruled out. Nevertheless, the direct enhancement of microbial killing by PR-39 still appears to be the most likely explanation for this phenotype.

The increasing number of antibiotic-resistant microorganisms has become a growing health care issue in both hospitals and the community (4, 30–32). This issue, coupled with the increasing frequency of invasive bacterial, viral, and fungal infections in the expanding community of immunocompromised patients, has inspired a search for alternatives to conventional antibiotics with desirable therapeutic indices (1, 6, 33–35). The development of medical therapies, such as prodrugs, that are less toxic and specifically target the location of pathology continues to be an important but challenging goal for medical research (36–38).

In this study, we present a cathelicidin in the form of its propeptide targeted to basal keratinocytes and demonstrate the potential therapeutic use of antimicrobial peptides in the skin. The PR-39 expressed in the K14-Cath-PR-39 transgenic mice acts as a prodrug because it remained apparently inactive until tissue injury with invasive bacterial infection. Although one might speculate that the source of these enzymes is keratinocytes, recruited leukocytes, or possibly bacteria themselves, more work to elucidate this issue is warranted. Nevertheless, while enhancing resistance against bacterial skin infection, the expression of the PR-39 precursor protected the skin against detrimental inflammation caused by the mature peptide. Therefore, the expression of a second cathelicidin propeptide in murine skin conferred protection against invasive bacterial infection, mimicking the strategies of precursor processing and expression of multiple cathelicidin genes that has evolved in other mammalian species.

1. Fernandez Guerrero, M. L., Ramos, J. M., Marrero, J., Cuenca, M., Fernandez Roblas, R. & de Gorgolas, M. (2003) *Int. J. Infect. Dis.* **7,** 46–52.
2. Wilson, B. A. & Salyers, A. A. (2002) *Curr. Opin. Biotechnol.* **13,** 267–274.
3. Schwenger, V., Mundlein, E., Dagrosa, E. E., Fahr, A. M., Zeier, M., Mikus, G. & Andrassy, K. (2002) *Infection* **30,** 257–261.
4. Gonzalez, A., Bischoff, T., Tallent, S., Sheke, G., Ostrowsky, B., Edmond, M. B. & Wenzel, R. P. (2003) *J. Hosp. Infect.* **55,** 156–157.
5. Healy, V. L., Park, I. S. & Walsh, C. T. (1998) *Chem. Biol.* **5,** 197–207.
6. Zhang, G., Ross, C. R. & Blecha, F. (2000) *Vet. Res.* **31,** 277–296.
7. Zaiou, M. & Gallo, R. L. (2002) *J. Mol. Med.* **80,** 549–561.
8. Zaiou, M., Nizet, V. & Gallo, R. L. (2003) *J. Invest. Dermatol.* **120,** 810–816.
9. Lehrer, R. I. & Ganz, T. (2002) *Curr. Opin. Hematol.* **9,** 18–22.
10. Gallo, R. L., Murakami, M., Ohtake, T. & Zaiou, M. (2002) *J. Allergy Clin. Immunol.* **110,** 823–831.
11. Nizet, V., Ohtake, T., Lauth, X., Trowbridge, J., Rudisill, J., Dorschner, R. A., Pestonjamasp, V., Piraino, J., Huttner, K. & Gallo, R. L. (2001) *Nature* **414,** 454–457.
12. Cole, A. M., Shi, J., Ceccarelli, A., Kim, Y. H., Park, A. & Ganz, T. (2001) *Blood* **97,** 297–304.
13. Wilson, C. L., Ouellette, A. J., Satchell, D. P., Ayabe, T., Lopez-Boado, Y. S., Stratman, J. L., Hultgren, S. J., Matrisian, L. M. & Parks, W. C. (1999) *Science* **286,** 113–117.
14. Bals, R., Weiner, D. J., Meegalla, R. L. & Wilson, J. M. (1999) *J. Clin. Invest.* **103,** 1113–1117.
15. Huang, H. J., Ross, C. R. & Blecha, F. (1997) *J. Leukocyte Biol.* **61,** 624–629.
16. Li, J., Post, M., Volk, R., Gao, Y., Li, M., Metais, C., Sato, K., Tsai, J., Aird, W., Rosenberg, R. D., *et al.* (2000) *Nat. Med.* **6,** 49–55.
17. Simon, D. & Ferretti, J. J. (1991) *FEMS Microbiol. Lett.* **66,** 219–224.
18. Vassar, R., Rosenberg, M., Ross, S., Tyner, A. & Fuchs, E. (1989) *Proc. Natl. Acad. Sci. USA* **86,** 1563–1567.
19. Gordon, J. W., Scangos, G. A., Plotkin, D. J., Barbosa, J. A. & Ruddle, F. H. (1980) *Proc. Natl. Acad. Sci. USA* **77,** 7380–7384.
20. Chomczynski, P. & Sacchi, N. (1987) *Anal. Biochem.* **162,** 156–159.
21. Murakami, M., Ohtake, T., Dorschner, R. A. & Gallo, R. L. (2002) *J. Dent. Res.* **81,** 845–850.
22. Betschel, S. D., Borgia, S. M., Barg, N. L., Low, D. E. & De Azavedo, J. C. (1998) *Infect. Immun.* **66,** 1671–1679.
23. Dorschner, R. A., Pestonjamasp, V. K., Tamakuwala, S., Ohtake, T., Rudisill, J., Nizet, V., Agerberth, B., Gudmundsson, G. H. & Gallo, R. L. (2001) *J. Invest. Dermatol.* **117,** 91–97.
24. Chon, J. H., Houston, M. M., Xu, C. & Chaikof, E. L. (2001) *J. Cell. Physiol.* **189,** 133–143.
25. Salzman, N. H., Ghosh, D., Huttner, K. M., Paterson, Y. & Bevins, C. L. (2003) *Nature* **422,** 522–526.
26. Ong, P. Y., Ohtake, T., Brandt, C., Strickland, I., Boguniewicz, M., Ganz, T., Gallo, R. L. & Leung, D. Y. (2002) *N. Engl. J. Med.* **347,** 1151–1160.
27. Agerberth, B., Lee, J. Y., Bergman, T., Carlquist, M., Boman, H. G., Mutt, V. & Jornvall, H. (1991) *Eur. J. Biochem.* **202,** 849–854.
28. Gallo, R. L., Ono, M., Povsic, T., Page, C., Eriksson, E., Klagsbrun, M. & Bernfield, M. (1994) *Proc. Natl. Acad. Sci. USA* **91,** 11035–11039.
29. Levy, O., Weiss, J., Zarember, K., Ooi, C. E. & Elsbach, P. (1993) *J. Biol. Chem.* **268,** 6058–6063.
30. Singh, N. (2001) *Clin. Microbiol. Infect.* **7,** Suppl. 2, 1–7.
31. Gomez-Lus, R. (1998) *Int. Microbiol.* **1,** 279–284.
32. Novak, R., Henriques, B., Charpentier, E., Normark, S. & Tuomanen, E. (1999) *Nature* **399,** 590–593.
33. Maertens, J., Vrebos, M. & Boogaerts, M. (2001) *Eur. J. Cancer Care* **10,** 56–62.
34. Johnson, R. A. (2000) *Semin. Cutan. Med. Surg.* **19,** 19–61.
35. Maschmeyer, G., Noskin, G. A., Ribaud, P. & Sepkowitz, K. A. (2000) *Oncology (Huntington, N.Y.)* **14,** 9–16.
36. Ng, A. W., Wasan, K. M. & Lopez-Berestein, G. (2003) *J. Pharm. Pharm. Sci.* **6,** 67–83.
37. Ferguson, M. J., Ahmed, F. Y. & Cassidy, J. (2001) *Drug Resist. Update* **4,** 225–232.
38. Lee, H. J., Cooperwood, J. S., You, Z. & Ko, D. H. (2002) *Arch. Pharm. Res.* **25,** 111–136.

IMMUNOLOGY